



Coastal submersions in the north-eastern Adriatic during the last 5200 years

David Kaniewski^{a,b,*}, Nick Marriner^c, Rachid Cheddadi^d, Christophe Morhange^{e,f,g}, Matteo Vacchi^h, Alessio Rovereⁱ, Sanja Faivre^j, Thierry Otto^k, Frédéric Luce^k, Marie-Brigitte Carre^l, Gaetano Benčić^m, Elise Van Campo^k

^a TRACES, UMR 5608 CNRS, Université Toulouse Jean Jaurès, Maison de la Recherche, 5 allées A. Machado, 31058 Toulouse Cedex 9, France

^b Université Paul Sabatier Toulouse 3, 118 Route de Narbonne, 31062 Toulouse cedex 9, France

^c CNRS, Théma, Université de Franche-Comté, UMR 6049, MSHE Ledoux, 32 rue Mégevand, 25030 Besançon Cedex, France

^d Université Montpellier II, CNRS-UM-IRD, ISEM, Montpellier, France

^e Aix Marseille Université, CNRS, IRD, INRAE, CEREGE, Aix-en-Provence, France

^f RIMS, The Leon Recanati Institute for Maritime Studies, University of Haifa, Mount Carmel, Haifa 3498838, Israel

^g Ecole Pratique des Hautes Etudes, EPHE, Les Patios Saint-Jacques 4-14 rue, Ferrus, 75014 Paris, France

^h Dipartimento di Scienze Della Terra, Università di Pisa, Via S. Maria, 53, 56126 Pisa, Italy

ⁱ University of Bremen, Marum, ZMT, D-28359 Bremen, Germany

^j University of Zagreb, Faculty of Science, Department of Geography, Marulićev trg 19/II, 10 000 Zagreb, Croatia

^k Laboratoire Ecologie Fonctionnelle et Environnement, Université de Toulouse, CNRS, INP, UPS, Toulouse cedex 9, France

^l Aix Marseille Université, CNRS, CCJ, Aix-en-Provence, France

^m Zavičajni muzej Poreštine / Museo del territorio parentino, Poreč/Parenzo, Croatia

ARTICLE INFO

Keywords:

Coastal submersions
Saltwater intrusions
Paleoclimate
Relative Sea-level rise
Coasts
Croatia
Adriatic
Mediterranean
Holocene

ABSTRACT

In the context of industrial-era global change, Mediterranean coastal areas are threatened by relative sea level (RSL) rise. Shifts in the drivers of coastal dynamics are forecasted to trigger changes in the frequency of flooding of low-lying areas, with significant effects on marine-coastal environments, societies, economy and urban systems. Here, we probe coastal floods in the eastern part of the Gulf of Venice (coastal Croatia) to understand the drivers of saltwater intrusions. We reconstructed RSL rise in the north-eastern Adriatic during the Holocene based on 43 RSL index points and analyzed the evolution of coastal submersions on the Istrian Peninsula for the last 5200 years based on inputs of marine components and increases in supratidal scrubs. We produced pollen-based climate reconstructions to analyze the potential effects of air temperature and precipitation changes on submersions. We investigated the response of precipitation and temperature to mid-late Holocene summer/winter insolation forcing and insolation-induced changes in sea surface temperatures (SSTs). We found that during periods of warmer SST, coastal flooding increased markedly. This process seems to have been initiated by warmer atmospheric temperatures that led to increases in summer evaporation, counterbalancing the effects of heavy precipitation during winter. As a result, freshwater flows into coastal areas were reduced and resulted in recurrent inputs of saltwater inland. Our study suggests that present-day climate drivers (increases in SSTs and air temperatures, and decreases in precipitation) will probably favour frequent coastal flooding, a process that will be amplified by RSL rise.

1. Introduction

Relative Sea Level (RSL) rise features prominently among the consequences of climate change (Nicholls et al., 2007; Kopp et al., 2014,

2017; Rovere et al., 2016). In 2017, more than 600 million people lived in coastal areas (less than 10 m above sea level) and nearly 2.4 billion people (~40% of the world's population) resided within 100 km of the coast (UN Ocean Conference, 2017). The coastal zone accounts for only

* Corresponding author at: TRACES, UMR 5608 CNRS, Université Toulouse Jean Jaurès, Maison de la Recherche, 5 allées A. Machado, 31058 Toulouse Cedex 9, France.

E-mail address: david.kaniewski@univ-tlse3.fr (D. Kaniewski).

<https://doi.org/10.1016/j.gloplacha.2021.103570>

Received 10 May 2021; Received in revised form 1 July 2021; Accepted 2 July 2021

Available online 6 July 2021

0921-8181/© 2021 Elsevier B.V. All rights reserved.

20% of all land area (CIESEN, 2000) but population densities in coastal regions are about three times higher than the global average. The risk of coastal flooding and increased saltwater intrusions on coastal areas therefore concerns at least ~10% of the world's population. In the Mediterranean, coastal flooding events are among the most feared hazards as the region is particularly vulnerable to the effects of ongoing climate change (Satta et al., 2017) with densely populated seaboard (Wolff et al., 2020) and mass tourism (Cortés-Jiménez, 2008), infrastructure and heritage sites (Reimann et al., 2018; Anzidei et al., 2020) situated close to the shore and with often limited adaptive capacity (Cramer et al., 2020). By 2025, ~174 million people will live in coastal areas, estuaries and deltas (~33% of the Mediterranean's population; Fabres, 2012). RSL rise and storm-related floods will make low-lying zones and coastal activities increasingly exposed to submersion and beaches vulnerable to erosion (Hzami et al., 2011), and aquifers more sensitive to saltwater intrusion (Nicholls et al., 2021).

Among the threatened areas in the northern Mediterranean, the Gulf of Venice has been identified as a hot spot according to the Coastal Vulnerability Index, the Coastal Exposure Index, and the Coastal Risk Index (Satta et al., 2017; Furlan et al., 2018, 2021). This situation is worrying as populations and coastal infrastructure in low-elevation areas will potentially face recurrent submersion events (Antonioli et al., 2017; Marsico et al., 2017; Bonaldo et al., 2020). UNESCO World Heritage sites such as the Episcopal Complex of Poreč, the Stato da Terra - Stato del Mar occidental, Aquileia, or Venice (Camuffo et al., 2014) will all be exposed to coastal flooding and erosion with RSL scenarios based on the Representative Concentration Pathways (RCP 2.6, RCP 4.5 and RCP 8.5; Reimann et al., 2018; Zanchettin et al., 2020). While the whole northern Adriatic coastal system seems vulnerable, analysis of future RSL rise and storm surges at a narrow geographic scale (north-western coast - northern coast - north-eastern coast) shows a more contrasting pattern and underlines the uncertainty behind the extent of RSL rise (regional forcings versus remote effects; Scarascia and Lionello, 2013), its impacts, and the severity of storm surges on either side of the Gulf of Venice (Lionello et al., 2012; Conte and Lionello, 2013; Kaniewski et al., 2016; Bonaldo et al., 2020). Bonaldo et al. (2020) also showed a shift in directional wave-energy contributions in the northern Adriatic resulting in a possible local increase in wave climate severity along the northern and north-eastern coasts. This process could be aggravated in northern Croatia by coastal subsidence amounting to 0.4 mm per year (Faivre et al., 2019a, 2021), which is coherent with the estimated 0.45 ± 0.6 mm per year subsidence in southern Croatia (Faivre et al., 2013; Shaw et al., 2018). Moreover, RSL changes for the last 1500 years along north-eastern coasts seem consistent with shifts in temperature and consequently with periods of rapid climate change (Faivre et al., 2019a).

Here, our aim is to investigate the environmental patterns that may have favoured coastal submersions and increased saltwater inputs inland during the last 5200 years in the north-eastern Adriatic (Istrian peninsula - Croatia, Fig. 1), one of the most vulnerable areas to present-day changes (Bonaldo et al., 2020). Our study explores the role of RSL rise, variations in Mediterranean SST, climate shifts and winter/summer insolation as potential forcing agents that may have promoted coastal submersions during the Mid-to-Late Holocene, and to infer whether present-day trends could play out in a similar manner. By trying to understand how all these environmental drivers may have acted conjointly during the past, this study seeks to identify the processes/patterns behind coastal flooding events.

2. Marine influence

The term "marine influence" in this study encompasses all the processes leading to increases in seawater in the coastal zones of Croatia (including coastal submersions with temporary flooding or permanent intrusion, and an increase in storm activity at the marine-terrestrial boundary). The difference between saltwater inundations and saltwater intrusions was made based on the pattern of coastal freshwater



Fig. 1. Geographical location of the Mirna River delta and the bay of Busuja in Croatia.

inputs. When coastal freshwater discharges are reduced, the saltwater penetrates inland and becomes a long-term intrusion. Inversely, when coastal freshwater flows increase, the saltwater only remains an inundation.

Saltwater in coastal areas, estuaries, and deltas today constitutes a pressing problem affecting the sustainability of freshwater resources (Alvarado-Aguilar et al., 2012; Mastrocicco et al., 2019; Bellafiore et al., 2021). Saltwater inputs in the hinterland has been proven to affect aquifers/karst springs by increasing salinity (Bonacci and Gabrić, 2007; Terzić et al., 2008; Brkić et al., 2020), with implications for the groundwater table and agricultural productivity (Terzić et al., 2008). Recent data from Italy's largest river delta (the Po Delta) suggests that changes driven by climate and RSL rise will accentuate, in the near future, saltwater intrusions in its surface waters (Bellafiore et al., 2021). Currently, these occur mostly during the summer season when warm and dry conditions lead to low freshwater discharges to coastal areas. Saltwater intrusions are nowadays exacerbated by aquifer over-exploitation for water supply and irrigation, land subsidence, RSL rise, and climate change, which contribute to diminished natural groundwater recharge (Bonacci and Roje-Bonacci, 1997; Botto et al., 2020).

3. Material and methods

3.1. RSL in north-eastern Adriatic

We reconstructed the sea-level evolution of the north-eastern Adriatic Sea by coupling the sea-level data available in Vacchi et al. (2016) with those produced by Covelli et al. (2006), Faivre et al. (2011, 2019a, 2019b), Furlani et al. (2011), Trincardi et al. (2011), and Trobec et al. (2018). We thus assembled a set of 43 RSL index points (points that constrain the palaeo mean sea-level (MSL) in space and time; Shennan et al., 2015; Fig. 2a-b) derived from radiocarbon-dated samples of fossil *Lithophyllum byssoides* rims in Premantura, Uboka, and Brseč (Croatia) and sediment cores taken from the Gulf of Trieste and along the Istrian coast (Fig. S1; map from Becker et al., 2009). All the radiocarbon ages

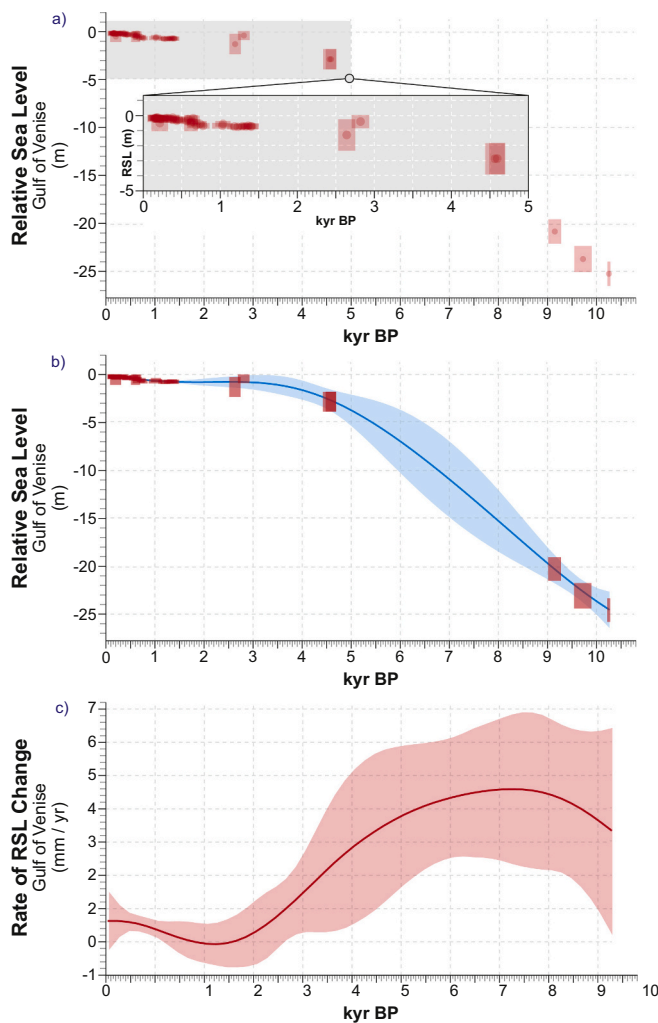


Fig. 2. Relative sea-level reconstruction of the north-eastern Adriatic Sea. a) The RSL history is based on 43 index points deriving from radiocarbon-dated samples of fossil *Lithophyllum byssoides* rims in Premantura, Uboka and Brseč (Croatia) and from sediment cores taken in the Gulf of Trieste and along the Istrian coasts. The dimensions of the red boxes denote the altitudinal and chronological errors associated with each index point. The inset corresponds to the last 5000 years. b) Estimates of the RSL with the 2-sigma errors. c) Rate of RSL change using the EIV IGP Model. (For interpretation of the references to colour in this figure legend, the reader is referred to the web version of this article.)

were re-calibrated into sidereal years with a 2σ range using the recent Calib-Rev 8.2. We employed the IntCal20 and Marine20 datasets for terrestrial and marine samples, respectively (Reimer et al., 2020). The regional average marine reservoir correction (ΔR) was applied for *L. byssoides* (ΔR of -209 ± 35 ^{14}C yr; Faivre et al., 2019b) and for shells from the Adriatic (ΔR of -59 ± 117 ^{14}C yr; Faivre et al., 2015) recalculated with Marine20 (Heaton et al., 2020). The indicative range (i.e. the relationship of the samples with respect to the former mean sea level) of each RSL index point was established according to Vacchi et al. (2016) and Faivre et al. (2019a-b). We then calculated the rate of RSL change using the Errors in Variables Integrated Gaussian Process (EIV IGP) Model (Fig. 2c). The EIV IGP was used to perform Bayesian inference on historical rates of RSL change (Cahill et al., 2016). The dataset is available in the supplement of this paper (Dataset S1).

3.2. Cores, chronology, and correlations

We collected two continuous cores from the delta of the Mirna River

(MIR IV, $45^{\circ}20'11.55''\text{N}$, $13^{\circ}39'30.29''\text{E}$, 1 m above current Mean Sea Level (MSL)) near Novigrad, Istrian peninsula (Kaniewski et al., 2016) and the bay of Busuja ($45^{\circ}15'55.05''\text{N}$, $13^{\circ}34'36.61''\text{E}$, 1 m below current MSL ($^{\text{b}}\text{MSL}$)) near Poreč, Istrian peninsula (Kaniewski et al., 2018; Fig. 1). The core MIR IV was drilled in the silty deposits of a micro-delta while the core S411 was drilled underwater in the silty-clay/sandy-clay deposits of the bay of Busuja, ~ 70 m from the present shoreline. These two cores were selected because they contain undisturbed sediment sequences. Their chronology (Fig. S2) is based on thirteen ^{14}C dates on short-lived samples (11 samples: terrestrial seeds; 2 samples: small leaves from terrestrial vegetation). All calibrated ages are provided with 2σ (95% probability) calibrated years BP (indicated as cal. BP in the text). A composite core was subsequently constructed based on radiometric (^{14}C dates), sedimentological and palaeoecological (layer of *Posidonia oceanica* debris and pollen analysis) correlations to build a sequence covering the last 5200 years (Fig. S3).

3.3. Biological data

The raw biological data derive from two studies (Kaniewski et al., 2016, 2018). Pollen data were initially shown as frequencies (%). Dinoflagellate cysts (marine plankton) were counted on pollen slides, reported as concentrations (cysts per cm^{-3}), and here provided as z-scores. Foraminifera, marine bivalves, and *Posidonia oceanica* debris were extracted from the same samples as the pollen grains and dinoflagellate cysts. These marine components (Foraminifera, marine bivalves) and *P. oceanica* debris were initially picked from the washed sediment fraction. The marine components were originally displayed as concentrations (remains per cm^{-3}) and transformed into z-scores. All data were analyzed using XL-Stat²⁰¹⁹ (<https://www.xlstat.com/fr/>) and the software package PAST, versions 2.17c and 4.03 (Hammer and Harper, 2006). A regular chronological interpolation (20-yr) was first applied to the dataset. Biological data were investigated using cluster analysis (descending type; Fig. S4). The cluster analysis was used to calculate a dendrogram, using branches as ecological distances between groups of taxa. The test was calculated using *Paired group* as an algorithm and *Correlation* as the similarity measure. Pollen taxa of each cluster were summed to derive vegetation dynamics (Fig. S5) from the supratidal zone (backshore scrubs) to the hinterland (mixed oak forest), referring to modern patches of vegetation (Fig. S4). The vegetation patterns are shown with their long-term trends displayed as sinusoidal regressions (phase Free, with $P_{\text{value}} < 0.001$) and smoothing splines (Fig. S5). The backshore scrubs assemblage was then transformed into z-scores.

The marine influence scores (Fig. 3) correspond to the average of two patterns. The first pattern was calculated by averaging the z-scores of the marine components, dinoflagellate cysts and backshore scrubs. The second pattern was calculated by excluding the backshore scrubs assemblage, which could be influenced by climate and/or marine influence. These two initial patterns appear as background in Fig. 3. The dataset is available in the supplement of this paper.

3.4. Pollen-based climate reconstruction

The pollen-based model used to reconstruct the climate variables (Figs. 3, 4) has been proven to provide coherent climate reconstructions (Cheddadi and Khater, 2016; Cheddadi et al., 2016, 2017; Kaniewski et al., 2019, 2020). We calculated two different models, with and without backshore scrubs. The main reconstructions presented in this study correspond to the average of the two models (which appear as background in Figs. 3, 4). All reconstructions are shown with their estimated errors, and with their long-term trends (Figs. 3, 4, 5). Summer precipitation was then used to calculate a freshwater discharge index (Fig. 6). All reconstructed climate data are available in the supplement of this paper.

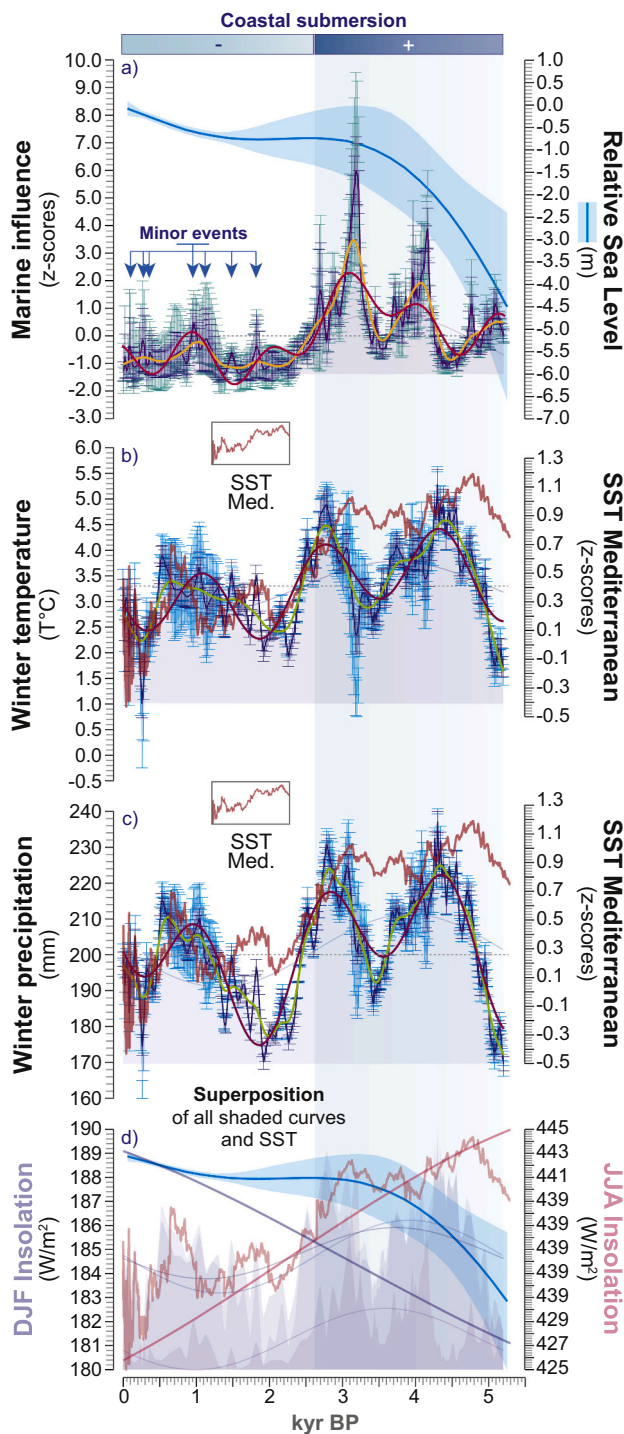


Fig. 3. Reconstruction of the marine influence for the last 5200 years compared with RSL, winter temperatures, winter precipitation and SSTs. a) Marine influence (z-scores) versus RSL rise (m). Red line: sinusoidal regression; orange line: smoothing spline. b) Winter temperature (°C) versus Mediterranean SSTs (z-scores; [Marriner et al., 2021](#)). Dark red line: sinusoidal regression; green line: smoothing spline. c) Winter precipitation (mm) versus Mediterranean SSTs (z-scores). Dark red line: sinusoidal regression; green line: smoothing spline. d) Superposition of all the curves (z-scores) with winter and summer insolation (W/m^2 ; [Laskar et al., 2004](#)). The long-term trends are displayed as sinusoidal regressions (phase Free, with $P_{value} < 0.001$; a, b, c and d) and smoothing splines (a, b, and c). (For interpretation of the references to colour in this figure legend, the reader is referred to the web version of this article.)

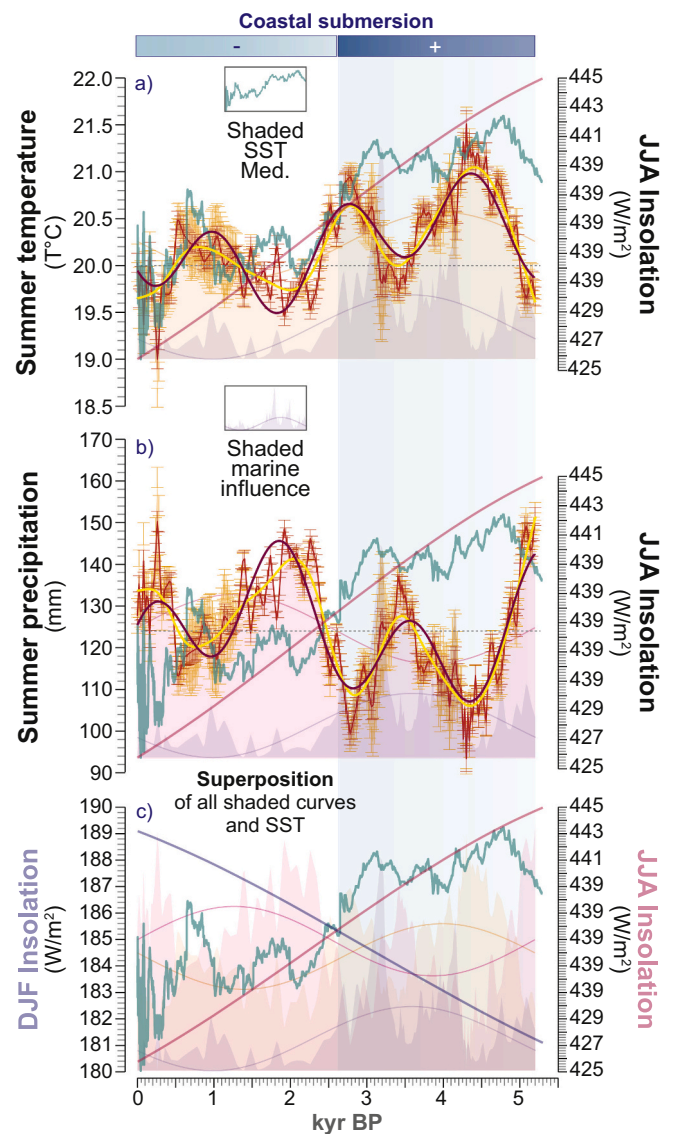


Fig. 4. Marine influence plotted against summer temperatures, summer precipitation, SSTs and insolation for the last 5200 years. a) Summer temperatures (°C) versus summer insolation (W/m^2 ; [Laskar et al., 2004](#)). The marine influence (z-scores) and the Mediterranean SSTs are shaded. Dark red line: sinusoidal regression; yellow line: smoothing spline. b) Summer precipitation (mm) versus summer insolation (W/m^2 ; [Laskar et al., 2004](#)). The marine influence (z-scores) and Mediterranean SSTs are shaded. Dark red line: sinusoidal regression; yellow line: smoothing spline. c) Superposition of all the curves (z-scores) with winter and summer insolation (W/m^2 ; [Laskar et al., 2004](#)). The long-term trends are displayed as sinusoidal regressions (phase Free, with $P_{value} < 0.001$; a, b, and c) and smoothing splines (a and b). (For interpretation of the references to colour in this figure legend, the reader is referred to the web version of this article.)

3.5. Agriculture

Agricultural activities were reconstructed by summing the cereals, cultivated trees and weeds (Fig. S4). The sum was then transformed into z-scores (Fig. 7). The initial threshold sizes used to discriminate cereals from other Poaceae (e.g. annulus thickness, pore diameter) are $47 \mu m$ for the grain diameter and $11 \mu m$ for the annulus diameter (e.g. [Joly et al., 2007](#); [Kaniewski et al., 2018](#)). Agricultural activities are shown with their long-term trends displayed as sinusoidal regressions (phase Free, with $P_{value} < 0.001$; Fig. 7). The potential impact of submersions on agriculture was tested by comparing the agricultural activities with a

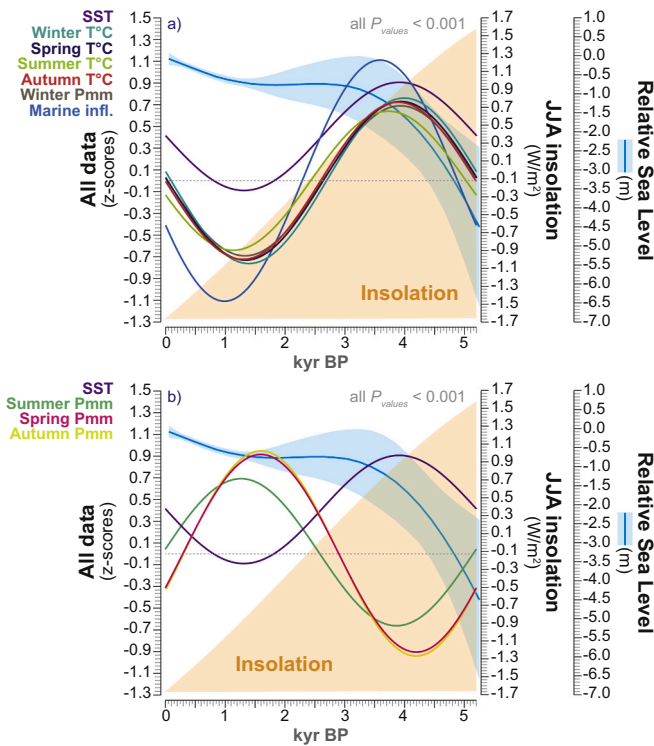


Fig. 5. Long-term trends in RSL, marine influence, temperatures, precipitation and summer insolation. a) Long-term trends (sinusoidal regression) in RSL, marine influence, temperatures (all seasons) and precipitation (winter) compared with SSTs (z-scores; Marriner et al., 2021) and summer insolation (W/m^2 ; Laskar et al., 2004). b) Long-term trends (sinusoidal regression) in RSL and precipitation (spring, summer and autumn) compared and contrasted with SSTs (z-scores) and summer insolation (W/m^2).

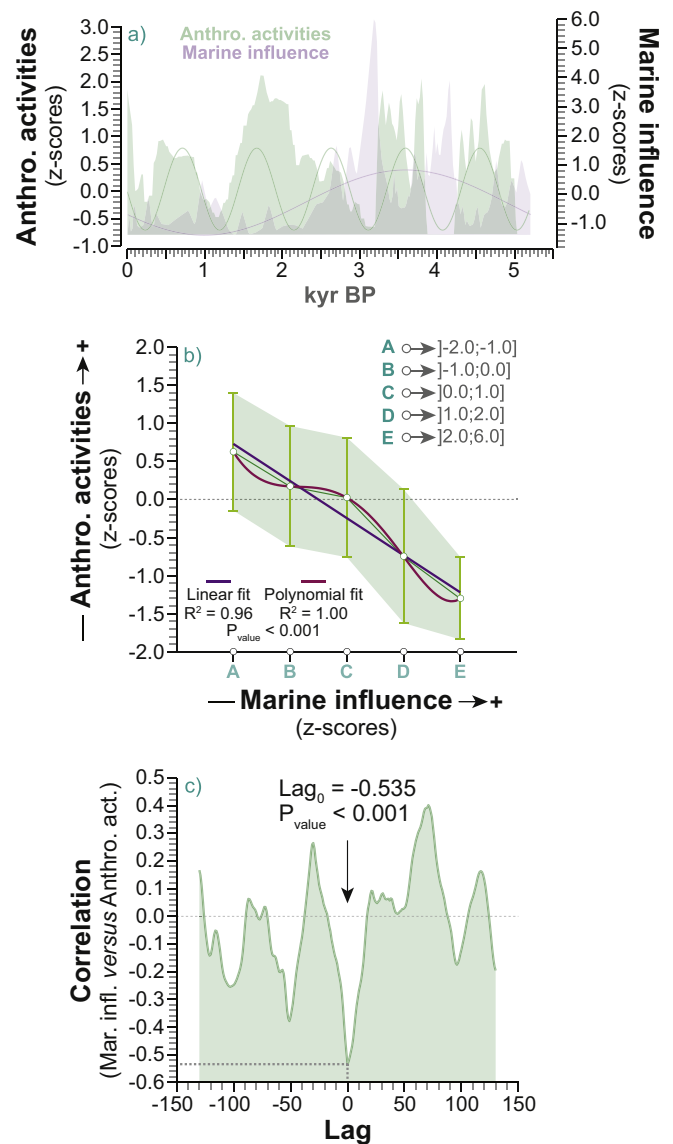


Fig. 7. Agricultural activities compared and contrasted with the marine influence during the last 5200 years. a) Agricultural activities (z-scores) plotted against marine influence (z-scores). The long-term trends are displayed as sinusoidal regressions (phase Free, with $P_{value} < 0.001$). b) The potential impact of submersions on agriculture was tested by comparing the agricultural activities with a continuous time series of marine influence. c) The cross-correlogram shows the link between the marine influence and the agricultural activities with the correlation coefficient at Lag_0 and the associated P_{value} .

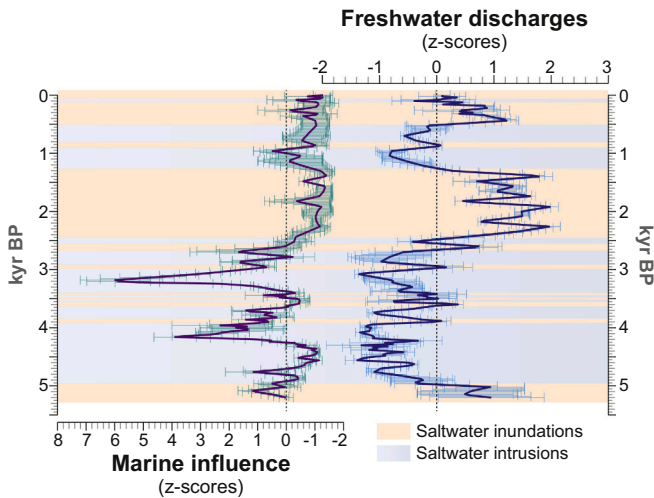


Fig. 6. Saltwater inundations versus saltwater intrusions. The marine influence (z-scores) is plotted against the freshwater discharge index (z-scores). The periods of saltwater intrusions are shaded in blue while the phases of saltwater inundations are shaded in orange. (For interpretation of the references to colour in this figure legend, the reader is referred to the web version of this article.)

continuous gradient of marine influence (Fig. 7a-b). To establish if anthropogenic activities were modulated by the coastal flooding, a cross correlation ($P < 0.05$) was calculated (Fig. 7c). The cross correlation assesses the time alignment of two time series by means of the correlation coefficient (CC). The time-series have been cross-correlated to

ascertain the best temporal match and the potential delay between the two time-series. The CC is then plotted as a function of the alignment position. This numerical approach is well adapted to detect and quantify potential links between environmental data and anthropogenic activities. Positive and negative correlation coefficients are considered, focusing on the Lag_0 value (with 0.5 or -0.5 as the significant threshold). Non-significant values indicate no correlation. All data are available in the supplement of this paper.

3.6. SST and insolation

The reconstruction of SST for the last 5200 years derives from a spatial average for the whole Mediterranean basin (Marriner et al., 2021). Summer and winter insolation scores (45° latitude) were extracted from (Laskar et al., 2004; Figs. 3, 4, 5). All data are available in

the supplement of this paper.

3.7. Further statistical analyses

A homogeneity test was applied to RSL, SST, insolation and marine influence data to detect potential shifts in their long-term dynamics (Fig. S6). The homogeneity test is based on a null hypothesis that a time series is homogenous. Possible alternative hypotheses such as change in distribution, changes in average or presence of trend can be detected and subdivided. Each change is highlighted and its average is indicated by “ μ ” (e.g. Kaniewski et al., 2020). A CABFAC/REGRESS analysis (Fig. S7) was used to test the potential weight of each factor (insolation, RSL, SST, temperature, precipitation, marine influence) in mediating the environmental signal (e.g. Kaniewski et al., 2020). The CABFAC factor analysis (Q-mode factor analysis) implements the classic method of factor analysis and environmental regression (CABFAC and REGRESS). The selected environmental data were regressed on the CABFAC factors using the second-order (parabolic) method, with cross terms. The environmental regression model (RMA) reports the observed values against the values reconstructed from the factors. The consistency of each reconstructed model is indicated by the coefficient of determination R^2 . The R^2 values were ordered from highest to lowest (Fig. S7).

4. Results

4.1. RSL rise for the last 10,000 years

A total of 43 RSL index points was used to frame the Holocene sea-level evolution of the north-eastern Adriatic (Fig. 2a). At 10,270 \pm 16.5 cal. BP, the index point places the RSL at 25.17 \pm 1.94 m^{bc}MSL (Fig. 2b) with a rising rate of 3.3 \pm 3 mm per year (Fig. 2c). The index points indicate that RSL rose rapidly until 5050 \pm 96.5 cal. BP (3.9 \pm 1.74 m^{bc}MSL and a rising rate of 2.8 \pm 2.2 mm per year), followed by a slowdown in the rising rates. Since this period, index points delineate a significant reduction in the rising rates during the last ~4000 years (4050 \pm 119 cal. BP: 1.68 \pm 1.02 m^{bc}MSL with a rising rate of 1.52 \pm 1.2 mm per year), when the total RSL variation was within 1.5 m^{bc}MSL (Fig. 2a-b). The significant slowdown in rising rates after ~5050 cal. BP is consistent with the progressive reduction in glacial meltwater inputs that were minimal during the last ~4000 years (Fig. 2c; Milne et al., 2005; Roy and Peltier, 2018).

4.2. Coastal submersions for the last 5200 years

According to our results, coastal submersions are defined by recurrent periods of higher activity during the last 5200 years (Fig. 3a), but with a stronger impact inland before 2580 \pm 65 cal. BP and lower since (Fig. S6). The main phase of increasing coastal submersions was recorded from 5200 \pm 60 to 2580 \pm 65 cal. BP with two peaks at 4180 \pm 65 cal. BP and 3180 \pm 70 cal. BP, which may correspond to increases in storminess (Kaniewski et al., 2016, 2018). When the RSL is superimposed on the coastal submersions, it appears that the major slowdown in RSL rise from 4200 \pm 119 to 2600 \pm 103 cal. BP is synchronous with the main phases of marine influence in the coastal area (Fig. S6). The tipping-point that marks the transition between high versus low coastal flooding also corresponds to a marked transition in the summer insolation, RSL rise and SST (Fig. S6), suggesting a link between all these parameters. This link is also highlighted by the CABFAC analysis which depicts the respective role of each parameter in the environmental signal (Fig. S7). The period 2680 \pm 65–760 \pm 70 cal. BP is marked by a general decrease in submersions with minor events at 1820 \pm 70, 1480 \pm 70, 1140 \pm 85 and 960 \pm 85 cal. BP (Fig. 3a). From 760 \pm 70 cal. BP to 475 \pm 70 cal. BP, episodes of marine influence occurred but not with the same intensity as those recorded during the period 5200 \pm 60–2580 \pm 65 cal. BP. The last events played out at 360 \pm 40, 260 \pm 15 and 100 \pm 45 cal. BP (Fig. 3a).

4.3. Climate

Phases of coastal submersions from 5200 \pm 60 to 2580 \pm 65 cal. BP mainly occurred during periods of warmer winter temperatures (Fig. 3b) and sustained winter precipitation (Fig. 3c). Temperatures are important as they were defined by the CABFAC analysis as the main parameter behind the observed changes (Fig. S7). The two main events (storms) seem to occur during cooler and slightly drier winters encompassed in these periods (Fig. 3b-c). The highest peak of submersion at 3180 \pm 70 cal. BP is linked to winter temperatures of 2.34 \pm 0.4 °C and winter precipitation of 200 \pm 3.3 mm while the averages for the period 5200–2580 cal. BP are respectively 3.64 \pm 0.3 °C and 207 \pm 2.7 mm. Warmer SSTs are also linked with the main phases of saltwater intrusions in the north-eastern Adriatic (Fig. 3b-c). Summer insolation seems to be a driver behind all these processes because the system seems to be less active during winter insolation (Fig. 3c).

Episodes of coastal submersions also occurred during years of warmer summer temperatures (Fig. 4a) and lower summer precipitation (Fig. 4b). The two major phases that correspond to storm events (peaks at 4180 \pm 65 cal. BP and 3180 \pm 70 cal. BP) occurred during years characterized by a slightly cooler but mostly drier summer season (Fig. 4c).

When all factors are pieced together, using only long-term trends (Fig. 5a-b), it appears that higher marine influence in the coastal area is linked with summer insolation, transgressive RSL, warm SSTs, warmer temperatures for all seasons, and stronger winter precipitation. Lower summer, spring and autumn precipitation also favoured coastal submersions. All the climatic parameters for each season are detailed in the supplementary material (Figs. S8, S9).

4.4. Saltwater inundations or intrusions?

The distinction between long-term processes (intrusion of saltwater) and short-term events (inundation) may be done using both the marine influence, precipitation and riverbank vegetation. One of the main parameters that nowadays controls the intrusion of saltwater in aquifers is the summer precipitation (Bonacci and Roje-Bonacci, 1997; Botto et al., 2020). Reconstructed summer precipitation was here coupled with macrophytes-helophytes and riparian trees to create an index of freshwater discharge (Fig. 6). The average of both time series (marine influence and freshwater discharges) was used to subdivide the signals into low versus high scores. We assume that flooding activity that lead to saltwater intrusions is attested by phases of freshwater discharges below average (Fig. 6). The periods where the freshwater discharges were above average correspond to a weakening of marine influence and are defined as coastal inundation by saltwater. The marine influence was compared and contrasted with the freshwater discharges and two main phases were defined (Fig. 6), divided by the tipping-point. Before the tipping-point (2580 \pm 65 cal. BP; Fig. S6), the area is mainly affected by saltwater intrusions resulting from important coastal flooding and low freshwater inputs (Fig. 6). After the tipping-point, the area seems to have been mainly affected by recurrent/permanent saltwater inundations due to higher inputs of freshwater to the coastal area and a weakening of all parameters favoring important coastal flooding (Fig. S6).

4.5. Agricultural activities and marine influence

The agricultural activities in coastal areas appear to be modulated by saltwater (Fig. 7a), as suggested for the modern period (Terzić et al., 2008). Each phase defined by significant activity in terms of marine influence (Fig. 6) is concomitant with a major decline in agriculture, suggesting saltwater intrusions, which probably affected aquifers by rising salinity, and further impacted the groundwater table. When the evolution of agricultural activities is compared and contrasted with marine influence, it is clear that saltwater modulates these activities (i.e. the more saltwater penetrates inland, the more these activities decline,

or even disappear, Fig. 7b-c). This suggests a causal link between the two processes (e.g. Bonacci and Gabrić, 2007; Terzić et al., 2008; Brkić et al., 2020).

5. Discussion

As emphasized by the International Panel on Climate Change (e.g. IPCC, 2007, 2014), present-day climate change effects are expected to substantially increase global mean sea level (Chang et al., 2011), significantly affecting erosion and flooding of coastal areas in the near future (Aucelli et al., 2017). This rise will also have a severe adverse effect on saltwater intrusion processes in coastal aquifers whereas the need for freshwater is increasing as burgeoning population levels require more water for their domestic, agricultural and industrial uses (Cominelli et al., 2009). While coastal freshwater resources are intensively used nowadays to meet this demand (Mollema et al., 2013), increasing efforts are being made to understand the consequences of environmental change for society, particularly for water resource management (García-Ruiz et al., 2011). In the dry Mediterranean basin, changes in water resources are particularly relevant as water availability is a limiting factor for economic development. Moreover, there is an unequivocal trend in the Mediterranean towards drier conditions (Guiot and Cramer, 2016). Climate models highlight rainfall changes, and the frequency and intensity of droughts have intensified since the 1950s (Gao and Giorgi, 2008). This situation will be exacerbated in the future (Giorgi and Lionello, 2008) as the Industrial-era increase in aridity has accentuated stress on already limited water resources, particularly in coastal regions where anthropogenic demands already exceed supply (Cramer et al., 2018).

5.1. Coastal flooding

Focussing on the last 5200 years, coastal flooding resulting in saltwater intrusions occurred several times on the Istrian peninsula, mainly during the period 5200 ± 60 to 2580 ± 65 cal. BP. These phases of coastal flooding seem to be triggered by several cumulative causes (Figs. 3, 4, S7). The main parameters identified correspond to RSL variability (rise and a slowdown of the rising rates during the Holocene; Fig. 2), warm SSTs until $\sim 3000 \pm 50$ cal. BP (Fig. 3), warmer atmosphere temperatures for each season (Figs. 3b, 4a, S7, S9), and drier conditions (Figs. 4b, S7, S8). This is correlated with summer insolation (Fig. 5) while increased winter insolation seems to have lowered the magnitude of coastal flooding. The main component behind coastal flooding and saltwater intrusions seem to be due to marine and atmospheric heat. Warmer atmospheric temperatures led to an increase in evaporation during summer in coastal areas, counterbalancing the effect of heavy precipitation during winter. This process reduced the freshwater discharges in coastal areas and resulted in recurrent intrusions of saltwater inland (Fig. 6).

The surface temperature and precipitation patterns seem to follow the variations in solar activity (Solanski et al., 2005; Vonmoos et al., 2006; Steinhilber et al., 2012), particularly the warmer (all seasons; Fig. S9) and drier (summer, spring, and autumn) interval that started ~ 5200 years ago and ended ~ 2580 years ago. This warmth was coupled with a probable steric effect of sea surface temperatures on RSL changes (Carillo et al., 2012), causing thermal expansion of sea waters and leading to RSL rise (Carillo et al., 2012; Cazenave and Le Cozannet, 2013). This increase was reinforced by land ice melt which only became minimal during the last ~ 4000 years (Roy and Peltier, 2018). This process probably favoured coastal submersions and saltwater intrusions.

During the period 5200 ± 60 to 2580 ± 65 cal. BP, Mediterranean SSTs show a phase of sustained warming. This plateau, defined by an average anomaly of 0.91 °C, initially starts at 9400 ± 50 and ends at 3000 ± 50 cal. BP (Marriner et al., submitted). After 3000 ± 50 cal. BP, the SSTs show an overall cooling trend (Marriner et al., 2021), resulting from an expansion of the Siberian High over Eurasia. These observations

are consistent with core AD91–17 from the southern Adriatic (Sangiorgi et al., 2003). When SSTs began cooling, after 3000 cal. BP, the marine influence on coastal areas was reduced (Fig. 3a-b), suggesting a link between the two processes (Fig. S7).

When the present-day parameters are compared with past data, it emerges that modern and predicted changes can lead to severe coastal submersions and increased saltwater inland in the near future. Atmospheric warming due to increased anthropogenic greenhouse gases (e.g. Giorgi and Lionello, 2008; Meinshausen et al., 2009) is strongly with glacial melting (e.g. Bocchiola and Diolaiuti, 2010; Diolaiuti et al., 2012), thermal expansion of sea waters (e.g. Tsimplis et al., 2008), RSL change (e.g. Galassi and Spada, 2014), and warm SST (e.g. Nykjaer, 2009). Mediterranean regional and global surface temperatures have significantly warmed for each season during the Industrial era (Milano et al., 2013; Lionello and Scarascia, 2018). Moreover, it has been suggested that areas situated along the northern seaboard of the Mediterranean region will be affected by a reduction in precipitation, mainly during summer, while they will not experience a significant drop in precipitation during winter (Lionello and Scarascia, 2018). It appears that all the present-day parameters seem to fit with what has been observed as factors favoring coastal submersions and saltwater inputs inland during the last 5200 years.

5.2. Storm events

The two main peaks of marine influence recorded at 4180 ± 65 cal. BP and 3180 ± 70 cal. BP correspond to important periods of floods resulting from recurrent storm surges in coastal Croatia during periods of low freshwater discharges (Figs. 3a, 6), leading to saltwater intrusions inland. Nowadays, severe storms usually affect coastal regions in the northern Adriatic during winter and, to a lesser extent, in summer (De Biasio et al., 2017). The storm surges that occur in the Adriatic Sea (e.g. Camuffo et al., 2000; Lionello et al., 2012), more frequently from autumn to spring, are regularly associated with the Scirocco, a steady, moist and warm south-easterly wind (Orlić et al., 1994), and to the Bora, a northeastern wind (Boldrin et al., 2009). These winds are also influenced by other forcing factors such as the barometric effect (associated with the spatial distribution of the atmospheric pressure over the Mediterranean Sea), rapid changes in the atmospheric pressure pattern, tides, and vertical land movement (e.g. Camuffo et al., 2000). Scirocco is channelled by the orography framing the basin and pushes the water towards the Gulf of Venice (Pirazzoli and Tomasin, 2002; Lionello et al., 2012; De Biasio et al., 2017). The Scirocco often lasts for days, moving significant amounts of water in the Gulf of Venice. Bora winds (Orlić et al., 1994, 2007) regularly generate gyres in surface coastal waters, depending on where the Bora's strongest offshore jets occur (Pullen et al., 2003; Signell et al., 2010). The sea-surface gyres, resulting from wind stresses, push waters westward and eastward in the Adriatic basin (Grisogono and Belušić, 2009). The component, which controls whether the western or the eastern coast is severely flooded, is dependent on the longitudinal wind, the Scirocco (Međugorac et al., 2015).

Severe storm episodes during the last 5200 years appear synchronous with warm SST but cooling surface temperatures (during each season) and drier winters (Fig. 3b-c). The highest marine influence activity during the period from 4180 ± 65 cal. BP to 3180 ± 70 cal. BP is associated with colder and drier winters and may correspond to an interval marked by a strengthened Bora effect over the Adriatic. Bora winds are dry, cold, and spatially inhomogeneous (Supić et al., 2012). It has been previously shown that lower winter temperatures may be caused by strengthened Bora winds over the Adriatic Sea (Sangiorgi et al., 2003). Moreover, it has also been shown that there is a tendency for a strong Bora (called "Dark Bora") to occur before the peak of the surge, being replaced by the Scirocco during the most intense phase of the storm events (Lionello et al., 2012). The strengthened storm activity during colder and drier periods may indicate when the Bora had a major influence over the northern Adriatic, with peaks marking the moment

when the Scirocco acted conjointly.

The climatic conditions that favoured severe storm episodes in the Adriatic during the last 5200 years (e.g. colder seasons with drier winters), are not attested nowadays or expected in the near future (Branković et al., 2012), suggesting a potential attenuation of storminess and saltwater intrusions resulting from these patterns. It has been further suggested that future changes in synoptic activity will lead to a reduction in Bora winds and to a lowest frequency of Scirocco events (Pasarić and Orlić, 2004). Additionally, a study of wind wave severity changes in the Adriatic Sea for the period 2070–2099 suggested milder conditions than the present-day pattern (Benetazzo et al., 2012). This reduced storm-surge activity could however be modulated by RSL rise and land subsidence, two factors that favour coastal submersions (Conte and Lionello, 2013), even with low severity storm events. While trends suggest a decline in storm activity in the near future, increases in wave severity may occur locally, depending on the local wind climate (Benetazzo et al., 2012).

5.3. Agricultural activities

Coastal submersions and saltwater intrusions (Fig. 6) have a strong impact on irrigated agriculture as portrayed during the last 5200 years (Fig. 7) as saline water cannot be used for irrigation (e.g. Baric et al., 2008). The drop in freshwater inputs led to important saltwater intrusions (Fig. 6) and a drop incoastal agriculture, mainly during the period before ~2580 cal. BP (Fig. 7).

An important prerequisite for the implementation of irrigation systems is the availability of freshwater which is nowadays one of the most limiting factors (Tadić, 2012). Water resources are estimated based on three criteria: quantity, quality and location (called “water potential”; Tadić, 2012). When drier conditions prevail (Fig. 4b, S8), precluding efficient aquifer recharge (e.g. Giambastiani et al., 2007), and saltwater intrusions increase (Figs. 3a, 6), the water potential is affected, with implications for agriculture in coastal areas (Fig. 7).

The consequences of saltwater intrusions in Croatia have been studied on the Blato aquifer (western side of the island of Korčula, southern Dalmatia; Terzić et al., 2008; Ilijanić et al., 2018), in the Neretva River Valley (southern Croatia; Zovko et al., 2013), in the Vrana Lake (Dalmatia; Rubinić and Katalinić, 2014), and at several aquifers from the Istrian peninsula to southern Croatia (Bonacci and Gabrić, 2007; Brkić et al., 2020). Studies tend to show that RSL rise, drier conditions, and human activities (e.g. pumping of freshwater) are the main forcing agents behind saltwater intrusions inland (e.g. Da Lio et al., 2015). In the near future, saltwater intrusions will probably increase, with repercussions for the economy, urban life, tourism, agriculture and daily life.

6. Conclusions

This study shows that coastal flooding and saltwater intrusions have had a major impact on the northeast Adriatic coastal areas over the past thousand years. Enhanced and recurrent submersions were triggered by several cumulative factors and processes such as RSL variability, warm SSTs, warmer atmospheric temperatures and drier conditions. The drivers behind past coastal submersion are similar to the modern and predicted changes, suggesting that present-day patterns may lead to severe submersion events and increased saltwater intrusions in the near future. The expected drop in freshwater availability due to saltwater intrusions, will be aggravated by important human activity in coastal areas, mainly high freshwater pumping and increasing pollution. Economic activities in coastal areas will therefore be affected as most of them rely on important freshwater availability (e.g. tourism, agriculture, industry). Inversely, severe storm events will probably be attenuated as climate conditions do not seem to be favorable to the development of extreme events. The real impact of milder storm events will be mainly determined by factors other than climate, such as coastal

subsidence and the rate of RSL rise.

Data availability

The data supporting our results are provided as Supplementary data to this article.

Declaration of Competing Interest

The authors declare that they have no known competing financial interests or personal relationships that could have appeared to influence the work reported in this paper.

Acknowledgments

We wish to thank the Centre Camille Jullian (Aix Marseille Université, CNRS), the Zavičajni musej Poreštine / Museo del territorio parentino (Poreč, Croatia), and the Croatian Science Foundation. A.R. and M.V. acknowledge PALSEA, a working group of the International Union for Quaternary Research (INQUA) and Past Global Changes (PAGES), which in turn received support from the Swiss Academy of Sciences and the Chinese Academy of Sciences. This work is a contribution to the French MITI CNRS (project URBMED), and the Croatian Science Foundation (project SEALeVeL no. HRZZ IP-2019-04-9445). We wish to thank the editor and three anonymous reviewers for their constructive comments, which have improved the quality of the manuscript.

Appendix A. Supplementary data

Supplementary data to this article can be found online at <https://doi.org/10.1016/j.gloplacha.2021.103570>.

References

- Alvarado-Aguilar, D., Jiménez, J.A., Nicholls, R.J., 2012. Flood hazard and damage assessment in the Ebro Delta (NW Mediterranean) to relative sea level rise. *Nat. Hazards* 62, 1301–1321. <https://doi.org/10.1007/s11069-012-0149-x>.
- Antonoli, F., Amorosi, A., Lo Presti, V., Mastroruzzi, G., Deiana, G., De Falco, G., Fontana, A., Fontolan, G., Lisco, S., Marsico, A., Moretti, M., Orrù, P.E., Sannino, G. M., Serpelloni, E., Vecchio, A., 2017. Sea-level rise and potential drowning of the Italian coastal plains: flooding risk scenarios for 2100. *Quat. Sci. Rev.* 158, 29–43. <https://doi.org/10.1016/j.quascirev.2016.12.021>.
- Anzidei, M., Doumaz, F., Vecchio, A., Serpelloni, E., Pizzimenti, L., Civico, R., Greco, M., Martino, G., Enei, F., 2020. Sea level rise scenario for 2100 AD in the heritage site of Pyrgi (Santa Severa, Italy). *J. Mar. Sci. Eng.* 8 (2), 64. <https://doi.org/10.3390/jmse8020064>.
- Aucelli, P.P.C., et al., 2017. Coastal inundation risk assessment due to subsidence and sea level rise in a Mediterranean alluvial plain (Vulturno coastal plain e southern Italy). *Estuar. Coast. Shelf Sci.* 198, 597–609. <https://doi.org/10.1016/j.ecss.2016.06.017>.
- Baric, A., Grbec, B., Bogner, D., 2008. Potential implications of sea-level rise for Croatia. *J. Coast. Res.* 24 (2), 299–305. <https://doi.org/10.2112/07A-0004>.
- Becker, J.J., Sandwell, D.T., Smith, W.H.F., Braud, J., Binder, B., Depner, J., Fabre, D., Factor, J., Ingalls, S., Kim, S.H., Ladner, R., Marks, K., Nelson, S., Pharaoh, A., Trimmer, R., Von Rosenberg, J., Wallace, G., Weatherall, P., 2009. Global bathymetry and elevation data at 30 arc seconds resolution: SRTM30-PLUS. *Mar. Geod.* 32, 355–371. <https://doi.org/10.1080/01490410903297766>.
- Bellafore, D., Ferrarin, C., Maicu, F., Manfè, F., Lorenzetti, G., Umjesser, G., Zaggia, L., Valle Levinson, A., 2021. Saltwater intrusion in a Mediterranean delta under a changing climate. *JGR Oceans* 126 (2). <https://doi.org/10.1029/2020JC016437>.
- Benetazzo, A., Fedele, F., Carniel, S., Ricchi, A., Bucchignani, E., Sclavo, M., 2012. Wave climate of the Adriatic Sea: a future scenario simulation. *Nat. Hazards Earth Syst. Sci.* 12, 2065–2076. <https://doi.org/10.5194/nhess-12-2065-2012>.
- Bocchiola, D., Diolaiuti, G., 2010. Evidence of climate change within the Adamello Glacier of Italy. *Theor. Appl. Climatol.* 100, 351–369. <https://doi.org/10.1007/s00704-009-0186-x>.
- Boldrin, A., Carniel, S., Giani, M., Marini, M., Bernardi Aubry, F., Campanelli, A., Grilli, F., Russo, A., 2009. Effects of bora wind on physical and biogeochemical properties of stratified waters in the northern Adriatic. *J. Geophys. Res.* 114, C08S92. <https://doi.org/10.1029/2008JC004837>.
- Bonacci, O., Gabrić, I., 2007. Investigations of the brackish karst springs on the Croatian Adriatic Sea coast. In: Sanford, W., Langevin, C., Polemio, M., Povinec, P. (Eds.), *A new focus on groundwater-seawater interactions*. IAHS Publ. 312, Wallingford UK, pp. 39–49.

- Bonacci, O., Roje-Bonacci, T., 1997. Sea water intrusion in coastal karst springs: example of the Blaž Spring (Croatia). *HSJ* 42 (1), 89–100. <https://doi.org/10.1080/02626669709492008>.
- Bonaldo, D., Bucchignani, E., Pomaro, A., Ricchi, A., Scavo, M., Carniel, S., 2020. Wind waves in the Adriatic Sea under a severe climate change scenario and implications for the coasts. *Int. J. Climatol.* 40, 5389–5406. <https://doi.org/10.1002/joc.6524>.
- Botto, A., Camporese, M., Salandini, P., 2020. Mitigation strategies to reduce saltwater intrusion in coastal aquifers: the testing site of Ca' Pasqua, Italy. EGU General Assembly 2020, EGU2020–13299. <https://doi.org/10.5194/egusphere-egu2020-13299>.
- Branković, Č., Patarčić, M., Güttler, I., Srnc, L., 2012. Near-future climate change over Europe with focus on Croatia in an ensemble of regional climate model simulations. *Clim. Res.* 52, 227–251. <https://doi.org/10.3354/cr01058>.
- Brkčić, Z., Kuhta, M., Hunjak, T., Larva, O., 2020. Regional isotopic signatures of groundwater in Croatia. *Water* 12, 1983. <https://doi.org/10.3390/w12071983>.
- Cahill, N., Kemp, A.C., Horton, B.P., Parnell, A.C., 2016. A Bayesian hierarchical model for reconstructing relative sea level: from raw data to rates of change. *Clim. Past* 12, 525–542. <https://doi.org/10.5194/cp-12-525-2016>.
- Camuffo, D., Secco, C., Brimblecombe, P., Martin-Vide, J., 2000. Sea storms in the Adriatic Sea and the Western Mediterranean during the last millennium. *Clim. Chang.* 46, 209–223. <https://doi.org/10.1023/A:1005607103766>.
- Camuffo, D., Bertolin, C., Schenali, P., 2014. Climate change, sea level rise and impact on monuments in Venice. In: Rogério-Candelera, M.A. (Ed.), *Science, Technology and Cultural Heritage*. CRC Press, London UK, pp. 1–17.
- Carillo, A., Sannino, G., Artale, V., Ruti, P.M., Calmanti, S., Dell'Aquila, A., 2012. Steric sea level rise over the Mediterranean Sea: present climate and scenario simulations. *Clim. Dyn.* 39, 2167–2184. <https://doi.org/10.1007/s00382-012-1369-1>.
- Cazenave, A., Le Cozannet, G., 2013. Sea level rise and its coastal impacts. *Earth's Future* 2, 15–34. <https://doi.org/10.1002/2013EF000188>.
- Chang, S.W., Clement, T.P., Simpson, M.J., Lee, K.K., 2011. Does sea-level rise have an impact on saltwater intrusion? *Adv. Water Resour.* 34 (10), 1283–1291. <https://doi.org/10.1016/j.advwatres.2011.06.006>.
- Cheddadi, R., Khater, C., 2016. Climate change since the last glacial period in Lebanon and the persistence of Mediterranean species. *Quat. Sci. Rev.* 150, 146–157. <https://doi.org/10.1016/j.quascirev.2016.08.010>.
- Cheddadi, R., Araújo, M.B., Maiorano, L., Edwards, M., Guisan, A., Carré, M., Chevalier, M., Pearson, P.B., 2016. Temperature range shifts for three European tree species over the last 10,000 years. *Front. Plant Sci.* 7, 1581. <https://doi.org/10.3389/fpls.2016.01581>.
- Cheddadi, R., Henrot, A.J., François, L., Boyer, F., Bush, M., Carré, M., Coissac, E., De Oliveira, P.E., Ficotola, F., Hambuckers, A., Huang, K., Lézine, A.M., Nourelbait, M., Rhoujati, A., Taberlet, P., Sarmiento, F., Abel-Schaad, D., Alba-Sánchez, F., Zheng, Z., 2017. Microrefugia, climate change, and conservation of *Cedrus atlantica* in the Rif Mountains, Morocco. *Front. Ecol. Evol.* 5, 114. <https://doi.org/10.3389/fevo.2017.00114>.
- CIESIN, 2000. Center for International Earth Science Information Network (CIESIN), International Food Policy Research Institute, and World Resources Institute. In: *Gridded Population of the World, Version 2*. Columbia University, Palisades, NY, CIESIN. Available: <http://sedac.ciesin.org/plue/gpw> (accessed November 2020).
- Cominelli, E., Galbiati, M., Tonelli, C., Bowler, C., 2009. Water: the invisible problem. *EMBO Rep.* 10 (7), 671–676. <https://doi.org/10.1038/embor.2009.148>.
- Conte, D., Lionello, P., 2013. Characteristics of large positive and negative surges in the Mediterranean Sea and their attenuation in future climate scenarios. *Glob. Planet. Change* 111, 159–173. <https://doi.org/10.1016/j.gloplacha.2013.09.006>.
- Cortés-Jiménez, I., 2008. Which type of tourism matters to the regional economic growth? The cases of Spain and Italy. *Int. J. Tourism Res.* 10, 127–139. <https://doi.org/10.1002/jtr.646>.
- Covelli, S., Fontolan, G., Faganeli, J., Ogrinc, N., 2006. Anthropogenic markers in the Holocene stratigraphic sequence of the Gulf of Trieste (northern Adriatic Sea). *Mar. Geol.* 230, 29–51. <https://doi.org/10.1016/j.margeo.2006.03.013>.
- Cramer, W., Guiot, J., Fader, M., Garrabou, J., Gattuso, J.P., Iglesias, A., Lange, M.A., Lionello, P., Llasat, M.C., Paz, S., Peñuelas, J., Snoussi, M., Toreti, A., Tsimplis, M.N., Xoplaki, E., 2018. Climate change and interconnected risks to sustainable development in the Mediterranean. *Nat. Clim. Chang.* 8, 972–980. <https://doi.org/10.1038/s41558-018-0299-2>.
- Cramer, W., Guiot, J., Tode, L., 2020. Climate change. In: *State of the Environment and Development in the Mediterranean (SOED 2020)*, United Nations Environment Program/Mediterranean Action Plan and Plan Bleu, pp. 57–82. Available: <https://p.lanbleu.org/en/soed-2020-state-of-environment-and-development-in-mediterranean/> (accessed November 2020).
- Da Lio, C., Carol, E., Kruse, E., Teatini, P., Tosi, L., 2015. Saltwater contamination in the managed low-lying farmland of the Venice coast, Italy: An assessment of vulnerability. *Sci. Total Environ.* 533, 356–369. <https://doi.org/10.1016/j.scitotenv.2015.07.013>.
- De Biasio, F., Bajo, M., Vignudelli, S., Umgiesser, G., Zecchetto, S., 2017. Improvements of storm surge forecasting in the Gulf of Venice exploiting the potential of satellite data: the ESA DUE eSurge-Venice project. *Eur. J. Remote Sens.* 50 (1), 428–441. <https://doi.org/10.1080/22797254.2017.1350558>.
- Diolaiuti, G., Bocchiola, D., D'agata, C., Smiraglia, C., 2012. Evidence of climate change impact upon glaciers' recession within the Italian Alps. The case of Lombardy glaciers. *Theor. Appl. Climatol.* 109, 429–445. <https://doi.org/10.1007/s00704-012-0589-y>.
- Fabres, J., 2012. United Nations Environment Program / Mediterranean Action Plan. In: *State of the Mediterranean marine and coastal environment, UNEP/MAP - Barcelona Convention*, Athens, 2012. Available: <https://www.grida.no/publications/192> (accessed November 2020).
- Faivre, S., Fouache, E., Ghilardi, M., Antonioli, F., Furlani, S., Kováčič, V., 2011. Relative sea level change in Istria (Croatia) during the last millennia. *Quat. Int.* 232, 132–143. <https://doi.org/10.1016/j.quaint.2010.05.027>.
- Faivre, S., Bakran-Petricioli, T., Horvatinić, N., Sironić, A., 2013. Distinct phases of relative sea level changes in the central Adriatic during the last 1500 years - influence of climatic variations? *Palaeogeogr. Palaeoclimatol. Palaeoecol.* 369, 163–174. <https://doi.org/10.1016/j.palaeo.2012.10.016>.
- Faivre, S., Bakran-Petricioli, T., Baresić, J., Horvatinić, N., 2015. New data on the marine radiocarbon reservoir effect in the Eastern Adriatic based on pre-bomb marine organisms from the intertidal zone and shallow sea. *Radiocarbon* 57, 527–538. https://doi.org/10.2458/azu_rc.57.18452.
- Faivre, S., Bakran-Petricioli, T., Baresić, J., Horvatić, D., Macario, K., 2019a. Relative sea-level change and climate change in the Northeastern Adriatic during the last 1.5 ka (Istria, Croatia). *Quat. Sci. Rev.* 222, 105909. <https://doi.org/10.1016/j.quascirev.2019.105909>.
- Faivre, S., Bakran-Petricioli, T., Baresić, J., Morhange, C., Borković, D., 2019b. Marine radiocarbon reservoir age of the coralline intertidal alga *Lithophyllum byssoides* in the Mediterranean. *Quat. Geochronol.* 51, 15–23. <https://doi.org/10.1016/j.quageo.2018.12.002>.
- Faivre, S., Bakran-Petricioli, T., Baresić, J., Horvatić, D., 2021. *Lithophyllum* rims as biological markers for constraining palaeoseismic events and relative sea-level variations during the last 3.3 ka on Lopud Island, southern Adriatic, Croatia. *Glob. Planet. Change* 202, 103517. <https://doi.org/10.1016/j.gloplacha.2021.103517>.
- Furlan, E., Torresan, S., Critto, A., Marcomini, A., 2018. Spatially explicit risk approach for multi-hazard assessment and management in marine environment: the case study of the Adriatic Sea. *Sci. Total Environ.* 618, 1008–1023. <https://doi.org/10.1016/j.scitotenv.2017.09.076>.
- Furlan, E., Dalla Pozza, P., Michetti, M., Torresan, S., Critto, A., Marcomini, A., 2021. Development of a Multi-Dimensional Coastal Vulnerability Index: assessing vulnerability to inundation scenarios in the Italian coast. *Sci. Total Environ.* 772, 144650. <https://doi.org/10.1016/j.scitotenv.2020.144650>.
- Furlani, S., Biolchi, S., Cucchi, F., Antonioli, F., Busetti, M., Melis, R., 2011. Tectonic effects on Late Holocene sea level changes in the Gulf of Trieste (NE Adriatic Sea, Italy). *Quat. Int.* 232, 144–157. <https://doi.org/10.1016/j.quaint.2010.06.012>.
- Galassi, G., Spada, G., 2014. Sea-level rise in the Mediterranean Sea by 2050: Roles of terrestrial ice melt, steric effects and glacial isostatic adjustment. *Glob. Planet. Change* 123, 55–66. <https://doi.org/10.1016/j.gloplacha.2014.10.007>.
- Gao, X., Giorgi, F., 2008. Increased aridity in the Mediterranean region under greenhouse gas forcing estimated from high resolution simulations with a regional climate model. *Glob. Planet. Change* 62, 195–209. <https://doi.org/10.1016/j.gloplacha.2008.02.002>.
- García-Ruiz, J.M., López-Moreno, J.I., Vicente-Serrano, S.M., Lasanta-Martínez, T., Beguería, S., 2011. Mediterranean water resources in a global change scenario. *Earth-Sci. Rev.* 105, 121–139. <https://doi.org/10.1016/j.earscirev.2011.01.006>.
- Giambastiani, B.M.S., Antonellini, M., Oude Essink, G.H.P., Stuurman, R.J., 2007. Saltwater intrusion in the unconfined coastal aquifer of Ravenna (Italy): a numerical model. *J. Hydrol.* 340, 91–104. <https://doi.org/10.1016/j.jhydrol.2007.04.001>.
- Giorgi, F., Lionello, P., 2008. Climate change projections for the Mediterranean region. *Glob. Planet. Change* 63, 90–104. <https://doi.org/10.1016/j.gloplacha.2007.09.005>.
- Grisogono, B., Belušić, D., 2009. A review of recent advances in understanding the meso and microscale properties of the severe Bora wind. *Tellus* 61A, 1–16. <https://doi.org/10.1111/j.1600-0870.2008.00369.x>.
- Guiot, J., Cramer, W., 2016. Climate change: the 2015 Paris Agreement thresholds and Mediterranean basin ecosystems. *Science* 354 (6311), 465–468. <https://doi.org/10.1126/science.aah5015>.
- Hammer, O., Harper, D., 2006. *Paleontological data analysis*. Blackwell, Oxford UK.
- Heaton, T.J., Köhler, P., Butzin, M., Bard, E., Reimer, R.W., Austin, W., Bronk Ramsey, C., Hughen, K.A., Kromer, B., Reimer, P.J., Adkins, J., Burke, A., Cook, M.S., Olsen, J., Skinner, L.C., 2020. Marine20—the marine radiocarbon age calibration curve (0–55,000 cal BP). *Radiocarbon* 62, 779–820. <https://doi.org/10.1017/RDC.2020.68>.
- Hzami, A., Heggy, E., Amrouni, O., Mahe, G., Maanan, M., Abdeljaouad, S., 2011. Alarming coastal vulnerability of the deltaic and sandy beaches of North Africa. *Sci. Rep.* 11, 2320. <https://doi.org/10.1038/s41598-020-77926-x>.
- Ilijanić, N., Miko, S., Ozren, H., Bakrač, K., 2018. Holocene environmental record from lake sediments in the Bokačakko blato karst polje (Dalmatia, Croatia). *Quat. Int.* 494, 66–79. <https://doi.org/10.1016/j.quaint.2018.01.037>.
- IPCC, 2007. Intergovernmental Panel on Climate Change, fourth Assessment Report (AR4). Climate Change 2007. Available: <https://www.ipcc.ch/assessment-report/ar4/> (accessed November 2020).
- IPCC, 2014. Intergovernmental Panel on Climate Change, fifth Assessment Report (AR5). Climate Change 2014: mitigation of climate change. Available: <https://www.ipcc.ch/report/ar5/syr/>.
- Joly, C., Barillé, L., Barreau, M., Mancheron, A., Visset, L., 2007. Grain and annulus diameter as criteria for distinguishing pollen grains of cereals from wild grasses. *Rev. Palaeobot. Palynol.* 146, 221–233. <https://doi.org/10.1016/j.revpalbo.2007.04.003>.
- Kaniewski, D., Marriner, N., Morhange, C., Faivre, S., Otto, T., Van Campo, E., 2016. Solar pacing of storm surges, coastal flooding and agricultural losses in the Central Mediterranean. *Sci. Rep.* 6, 25197. <https://doi.org/10.1038/srep25197>.
- Kaniewski, D., Marriner, N., Morhange, C., Rius, D., Carre, M.B., Faivre, S., Van Campo, E., 2018. Croatia's Mid-Late Holocene (5200–3200 BP) coastal vegetation shaped by human societies. *Quat. Sci. Rev.* 200, 334–350. <https://doi.org/10.1016/j.quascirev.2018.10.004>.
- Kaniewski, D., Marriner, N., Cheddadi, R., Morhange, C., Bretschneider, J., Jans, G., Otto, T., Luce, F., Van Campo, E., 2019. Cold and dry outbreaks in the eastern

- Mediterranean 3200 years ago. *Geology* 47, 933–937. <https://doi.org/10.1130/G46491.1>.
- Kaniewski, D., Marriner, N., Cheddadi, R., Morhange, C., Cau Ontiveros, M.A., Fornós, J. J., Giaime, M., Trichon, V., Otto, T., Luce, F., Van Campo, E., 2020. Recent anthropogenic climate change exceeds the rate and magnitude of natural Holocene variability on the Balearic Islands. *Anthropocene* 32, 100268. <https://doi.org/10.1016/j.ancene.2020.100268>.
- Kopp, R.E., Horton, R.M., Little, C.M., Mitrovica, J.X., Oppenheimer, M., Rasmussen, D. J., Strauss, B.H., Tebaldi, C., 2014. Probabilistic 21st and 22nd century sea-level projections at a global network of tide-gauge sites. *Earth's Future* 2, 383–406. <https://doi.org/10.1002/2014EF000239>.
- Kopp, R.E., DeConto, R.M., Bader, D.A., Hay, C.C., Horton, R.M., Kulp, S., Oppenheimer, M., Pollard, D., Strauss, B.H., 2017. Evolving understanding of Antarctic ice-sheet physics and ambiguity in probabilistic sea-level projections. *Earth's Future* 5, 1217–1233. <https://doi.org/10.1002/2017EF000663>.
- Laskar, J., Robutel, P., Joutel, F., Gastineau, M., Correia, A.C.M., Levrard, B., 2004. A long-term numerical solution for the insolation quantities of the Earth. *A&A* 428, 261–285. <https://doi.org/10.1051/0004-6361:20041335>.
- Lionello, P., Scarascia, L., 2018. The relation between climate change in the Mediterranean region and global warming. *Reg. Environ. Chang.* 18, 1481–1493. <https://doi.org/10.1007/s10113-018-1290-1>.
- Lionello, P., Cavaleri, L., Nissen, K.M., Pino, C., Raicich, F., Ulbrich, U., 2012. Severe marine storms in the Northern Adriatic: characteristics and trends. *Phys. Chem. Earth* 40–41, 93–105. <https://doi.org/10.1016/j.pce.2010.10.002>.
- Marriner, N., Kaniewski, D., Pourkerman, M., Devillers, B., 2021. Anthropocene tipping point reverses long-term Holocene cooling of the Mediterranean Sea: a meta-analysis of the basin's Sea Surface Temperature records. Submitted to *Earth-Sci. Rev.*
- Marsico, A., Lisco, S., Lo Presti, V., Antonoli, F., Amorosi, A., Anzidei, M., Deiana, G., De Falco, G., Fontana, A., Fontolan, G., Moretti, M., Orrù, P.E., Serpelloni, E., Sannino, G., Vecchio, A., Mastronuzzi, G., 2017. Flooding scenario for four Italian coastal plains using three relative sea level rise models. *J. Maps* 13 (2), 961–967. <https://doi.org/10.1080/17445647.2017.1415989>.
- Mastrocicco, M., Busico, G., Colombani, N., Vigliotti, M., Ruberti, D., 2019. Modelling actual and future seawater intrusion in the Variconi coastal wetland (Italy) due to climate and landscape changes. *Water* 11, 1502. <https://doi.org/10.3390/w11071502>.
- Medugorac, I., Pasarić, M., Orlić, M., 2015. Severe flooding along the eastern Adriatic coast: the case of 1 December 2008. *Ocean Dyn.* 65, 817–830. <https://doi.org/10.1007/s10236-015-0835-9>.
- Meinshausen, M., Meinshausen, N., Hare, W., Raper, S.C.B., Frieler, K., Knutti, R., Frame, D.J., Allen, M.R., 2009. Greenhouse-gas emission targets for limiting global warming to 2°C. *Nature* 458, 1158–1163. <https://doi.org/10.1038/nature08017>.
- Milano, M., Ruelland, D., Fernandez, S., Dezetter, A., Fabre, J., Servat, E., Fritsch, J.M., Ardoin-Bardin, S., Thivet, G., 2013. Current state of Mediterranean water resources and future trends under climatic and anthropogenic changes. *HSJ* 58 (3), 498–518. <https://doi.org/10.1080/02626667.2013.774458>.
- Milne, G.A., Long, A.J., Bassett, S.E., 2005. Modeling Holocene relative sea-level observations from the Caribbean and South America. *Quat. Sci. Rev.* 24, 1183–1202. <https://doi.org/10.1016/j.quascirev.2004.10.005>.
- Mollema, P.N., Antonelli, M., Dinelli, E., Gabbianelli, G., Greggio, N., Stuyfzand, P.J., 2013. Hydrochemical and physical processes influencing salinization and freshening in Mediterranean low-lying coastal environments. *Appl. Geochem.* 34, 207–221. <https://doi.org/10.1016/j.apgeochem.2013.03.017>.
- Nicholls, R.J., Wong, P.P., Burkett, V.R., Codignotto, J.O., Hay, J.E., McLean, R.F., Ragoonaden, S., Woodroffe, C.D., 2007. Coastal systems and low-lying areas. In: Parry, M.L., Canziani, O.F., Palutikof, J.P., van der Linden, P.J., Hanson, C.E. (Eds.), *Climate change 2007: impacts, adaptation and vulnerability. Contribution of Working Group II to the Fourth Assessment Report of the Intergovernmental Panel on Climate Change*. Cambridge University Press, Cambridge UK, pp. 315–356.
- Nicholls, R.J., Lincke, D., Hinkel, J., Brown, S., Vafeidis, A.T., Meysing, B., Hanson, S. E., Merkens, J.L., Fang, J., 2021. A global analysis of subsidence, relative sea-level change and coastal flood exposure. *Nat. Clim. Chang.* 1–5. <https://doi.org/10.1038/s41558-021-00993-z>.
- Nykjaer, L., 2009. Mediterranean Sea surface warming 1985–2006. *Clim. Res.* 39, 1117. <https://doi.org/10.3354/cr00794>.
- Orlić, M., Kuzmić, M., Pasarić, Z., 1994. Response of the Adriatic Sea to the bora and sirocco forcing. *Contin. Shelf Res.* 14, 91–116. [https://doi.org/10.1016/0278-4343\(94\)90007-8](https://doi.org/10.1016/0278-4343(94)90007-8).
- Orlić, M., Dadić, V., Grbec, B., Leder, N., Marki, A., Matic, F., Mihanović, H., Paklar, G.B., Pasarić, M., Pasarić, Z., Vilibić, I., 2007. Wintertime buoyancy forcing, changing seawater properties, and two different circulation systems produced in the Adriatic. *J. Geophys. Res.* C3, 1–21. <https://doi.org/10.1029/2005JC003271>.
- Pasarić, M., Orlić, M., 2004. Meteorological forcing of the Adriatic: present vs. projected climate conditions. *Geofizika* 21, 69–87. <https://hrcak.srce.hr/17008>.
- Pirazzoli, P.A., Tomasin, A., 2002. Recent evolution of surge-related events in the northern Adriatic area. *J. Coast. Res.* 18, 537–554. <https://www.jstor.org/stable/4299101>.
- Pullen, J., Doyle, J.D., Hodur, R., Ogston, A., Book, J.W., Perkins, H., Signell, R., 2003. Coupled ocean-atmosphere nested modeling of the Adriatic Sea during winter and spring 2001. *J. Geophys. Res.* 108, 3320. <https://doi.org/10.1029/2003JC001780>.
- Reimann, L., Vafeidis, A.T., Brown, S., Hinkel, J., Tol, R.S.J., 2018. Mediterranean UNESCO World Heritage at risk from coastal flooding and erosion due to sea-level rise. *Nat. Commun.* 9, 416. <https://doi.org/10.1038/s41467-018-06645-9>.
- Reimer, P.J., Austin, W.E.N., Bard, E., Bayliss, A., Blackwell, P.G., Bronk Ramsey, C., Butzin, M., Cheng, H., Edwards, R.L., Friedrich, M., Grootes, P.M., Guilderson, T.P., Hajdas, I., Heaton, T.J., Hogg, A.G., Hughen, K.A., Kromer, B., Manning, S.W., Muscheler, R., Palmer, J.G., Pearson, C., van der Plicht, J., Reimer, R.W., Richards, D.A., Scott, E.M., Southon, J.R., Turney, C.S.M., Wacker, L., Adolphi, F., Büntgen, U., Capano, M., Fahrni, S., Fogtmann-Schulz, A., Friedrich, R., Kudsk, S., Miyake, F., Olsen, J., Reinig, F., Sakamoto, M., Sookdeo, A., Talamo, S., 2020. The IntCal20 Northern Hemisphere radiocarbon calibration curve (0–55 cal kBP). *Radiocarbon* 62, 725–757. <https://doi.org/10.1017/RDC.2020.41>.
- Rovere, A., Stocchi, P., Vacchi, M., 2016. Eustatic and relative sea level changes. *Curr. Clim. Chang. Rep.* 2, 221–231. <https://doi.org/10.1007/s40641-016-0045-7>.
- Roy, K., Peltier, W.R., 2018. Relative sea level in the Western Mediterranean basin: a regional test of the ICE-7G NA (VM7) model and a constraint on Late Holocene Antarctic deglaciation. *Quat. Sci. Rev.* 183, 76–87. <https://doi.org/10.1016/j.quascirev.2017.12.021>.
- Rubinić, J., Katalinić, A., 2014. Water regime of Vrana Lake in Dalmatia (Croatia): changes, risks and problems. *HSJ* 59 (10), 1908–1924. <https://doi.org/10.1080/02626667.2014.946417>.
- Sangiorgi, F., Capotondi, L., Comorbou Nebout, N., Vigliotti, L., Brinkhuis, H., Giunta, S., Lotter, A.F., Morigi, C., Negri, A., Reichert, G.J., 2003. Holocene seasonal sea-surface temperature variations in the southern Adriatic Sea inferred from a multiproxy approach. *J. Quat. Sci.* 18 (8), 723–732. <https://doi.org/10.1002/jqs.782>.
- Satta, A., Puddu, M., Venturini, S., Giupponi, C., 2017. Assessment of coastal risks to climate change related impacts at the regional scale: the case of the Mediterranean region. *Int. J. Disaster Risk Reduct.* 24, 284–296. <https://doi.org/10.1016/j.ijdrr.2017.06.018>.
- Scarascia, L., Lionello, P., 2013. Global and regional factors contributing to the past and future sea level rise in the Northern Adriatic Sea. *Glob. Planet. Change* 106, 51–63. <https://doi.org/10.1016/j.gloplacha.2013.03.004>.
- Shaw, T.A., Plater, A.J., Kirby, J.R., Roy, K., Holgate, S., Tutman, P., Cahill, N., Horton, B.P., 2018. Tectonic influences on late Holocene relative sea levels from the central-eastern Adriatic coast of Croatia. *Quat. Sci. Rev.* 200, 262–275. <https://doi.org/10.1016/j.quascirev.2018.09.015>.
- Shennan, I., Long, A.J., Horton, B.P., 2015. *Handbook of Sea-Level Research*. John Wiley & Sons, Chichester UK.
- Signell, R.P., Chignati, J., Horstmann, J., Doyle, J.D., Pullen, J., Askari, F., 2010. High-resolution mapping of Bora winds in the northern Adriatic Sea using synthetic aperture radar. *J. Geophys. Res.* 115, C04020. <https://doi.org/10.1029/2009JC005524>.
- Solanski, S.K., Usoskin, I.G., Kromer, B., Schüssler, M., Beer, J., 2005. Unusual activity of the Sun during recent decades compared to the previous 11,000 years. *Nature* 431, 1084–1087. <https://doi.org/10.1038/nature02995>.
- Steinilber, F., Abreu, J.A., Beer, J., Brunner, I., Christl, M., Fischer, H., Heikkilä, U., Kubik, P.W., Mann, M., McCracken, K.G., Miller, H., Miyahara, H., Oerter, H., Wilhelm, F., 2012. 9,400 years of cosmic radiation and solar activity from ice cores and tree rings. *Proc. Natl. Acad. Sci. U. S. A.* 109 (16), 5967–5971. <https://doi.org/10.1073/pnas.1118965109>.
- Supić, N., Kraus, R., Kuzmić, M., Paschini, E., Precali, R., Russoc, A., Vilibić, I., 2012. Predictability of northern Adriatic winter conditions. *J. Mar. Syst.* 90 (1), 42–57. <https://doi.org/10.1016/j.jmarsys.2011.08.008>.
- Tadić, L., 2012. Criteria for evaluation of agricultural land suitability for irrigation in Osijek County Croatia. In: Kumar, M. (Ed.), *Problems, Perspectives and Challenges of Agricultural Water Management*. IntechOpen, London UK, pp. 311–332.
- Terzić, J., Marković, T., Pekaš, Ž., 2008. Influence of sea-water intrusion and agricultural production on the Blato Aquifer, Island of Korčula, Croatia. *Environ. Geol.* 54, 719–729. <https://doi.org/10.1007/s00254-007-0841-4>.
- Trincardi, F., Argani, A., Correggiari, A., Fogliani, F., Rovere, M., Angeletti, L., Asioli, A., Campiani, E., Cattaneo, A., Gallerani, A., Piva, A., Remia, A., Ridente, D., Taviani, M., 2011. Note illustrative della Carta Geologica dei mari italiani alla scala 1:250.000 foglio NL 33-7 Venezia, 151. In: Istituto Superiore per la Protezione e la Ricerca Ambientale, Servizio Geologico d' Italia, Roma, Italy.
- Trobec, A., Busetti, M., Zgur, F., Baradello, L., Babich, A., Cova, A., Gordini, E., Romeo, R., Tomini, I., Poglajen, S., Diviaco, P., Vrabc, M., 2018. Thickness of marine Holocene sediment in the Gulf of Trieste (northern Adriatic Sea). *Earth Syst. Sci. Data* 10, 1077–1092. <https://doi.org/10.5194/essd-10-1077-2018>.
- Tsimplis, M.N., Marcos, M., Somot, S., 2008. 21st century Mediterranean Sea level rise: Steric and atmospheric pressure contributions from a regional model. *Glob. Planet. Change* 63, 105–111. <https://doi.org/10.1016/j.gloplacha.2007.09.006>.
- United Nations Ocean Conference, 2017. Sustainable Development Goal 14. Available: <https://oceanconference.un.org/documents> (accessed November 2020).
- Vacchi, M., Marriner, N., Morhange, C., Spada, G., Fontana, A., Rovere, A., 2016. Multiproxy assessment of Holocene relative sea-level changes in the western Mediterranean: sea level variability and improvements in the definition of the isostatic signal. *Earth-Sci. Rev.* 155, 172–197. <https://doi.org/10.1016/j.earscirev.2016.02.002>.
- Vonmoos, M., Beer, J., Muscheler, R., 2006. Large variations in Holocene solar activity: Constraints from 10Be in the Greenland Ice Core Project ice core. *J. Geophys. Res.* 111, A10105. <https://doi.org/10.1029/2005JA011500>.

- Wolff, C., Nikolettopoulos, T., Hinkel, J., Vafeidis, A.T., 2020. Future urban development exacerbates coastal exposure in the Mediterranean. *Scient. Rep* 10, 14420. <https://doi.org/10.1038/s41598-020-70928-9>.
- Zanchettin, D., Bruni, S., Raicich, F., Lionello, P., Adloff, F., Androsov, A., Antonioli, F., Artale, V., Carminati, E., Ferrarin, C., Fofonova, V., Nicholls, R.J., Rubinetti, S., Rubino, A., Sannino, G., Spada, G., Thiéblemont, R., Tsimplis, M., Umgiesser, G., Vignudelli, S., Wöppelmann, G., Zerbini, S., 2020. Sea-level rise in Venice: historic and future trends. *Nat. Hazards Earth Syst. Sci. Disc.* 1–56. <https://doi.org/10.5194/nhess-2020-351>.
- Zovko, M., Romić, D., Romić, M., Ondrašek, G., 2013. Soil and water management for sustained agriculture in alluvial plains and flood plains exposed to salinity: A case of Neretva River Valley. In: Ahmad, P., Azooz, M., Prasad, M. (Eds.), *Ecophysiology and Responses of Plants under Salt Stress*. Springer, New York, pp. 473–494.